Inorganic Chemistry

Article

Spin Crossover Behavior in the Iron(II)–2-pyridyl[1,2,3]triazolo[1,5-*a*]pyridine System: X-ray Structure, Calorimetric, Magnetic, and Photomagnetic Studies

Virginie Niel,[†,1a] Ana B. Gaspar,[†,1a] M. Carmen Muñoz,[1b] Belén Abarca,[1c] Rafael Ballesteros,[1c] and José Antonio Real*,[1a]

Institut de Ciencia Molecular/Departament de Química Inorgánica, Universitat de València, Doctor Moliner 50, 46100 Burjassot, Spain, Departament de Física Aplicada, Universitat Politècnica de València, Camino de Vera s/n, 46071, Valencia, Spain, and Departament de Química Orgánica de la Universitat de València, Avda. Vicente Andrés Estellés s/n, 46100 Burjassot, Spain

Compounds [Fe(tzpy)$_3$](BF$_4$)$_2$ (**1**), [Fe(tzpy)$_2$(NCS)$_2$]·S (S = 2CHCl$_3$ (**2**), H$_2$O (**3**)), and [Fe(tzpy)$_2$(NCSe)$_2$] (**4**) (tzpy is 3-(2-pyridyl)[1,2,3]triazolo[1,5-*a*]pyridine) have been synthesized and characterized. **1** crystallizes in the monoclinic noncentrosymmetric system, *Cc* space group, *Z* = 4, with *a* = 11.4680(6) Å, *b* = 27.449(2) Å, *c* = 12.4510(8) Å, *β* = 108.860(5)°, *V* = 3709.0(4) Å^3, and *T* = 293(2) K. The structure consists of mononuclear [Fe(tzpy)$_3$]$^{2+}$ diamagnetic species, which stack via *π*-interactions. Disordered BF$_4^-$ anions fill the voids generated by complex cations. **2** crystallizes in the triclinic system, *P*$\bar{1}$ space group, *Z* = 1, with *a* = 8.3340(4) Å, *b* = 8.6520(4) Å, *c* = 11.6890(6) Å, α = 89.113(2)°, *β* = 81.612(2)°, *γ* = 77.803(2)°, *V* = 814.90(7) Å^3, and *T* = 293(2) K. The structure consists of mononuclear [Fe(tzpy)$_2$(NCS)$_2$] neutral species, which interact each other via *π*-staking defining layers separated by two-dimensional arrays of CHCl$_3$. The average Fe–N bond distance, 2.176(3) Å, corresponds to what is expected for an iron(II) ion in the high-spin state. Compounds **2**–**4** undergo thermal-driven spin conversion. The regular solution model was applied to account for the corresponding to thermodynamic parameters. The intermolecular interaction parameter, the characteristic temperature, and the enthalpy and entropy changes associated with the spin conversion were estimated as Γ = 0.86 (**2**), 0.89 (**3**), and 3.79 (**4**) kJ mol^{-1}, $T_{1/2}$ = 75 (**2**), 118 (**3**), and 251 K (**4**), Δ*H* = 3.67 (**2**) and 4.08 (**3**) kJ mol^{-1}, and Δ*S* = 34 (**2**) and 34.5 (**3**) J K^{-1} mol^{-1}. Δ*H* = 8.75 kJ mol^{-1} and Δ*S* = 34.8 J K^{-1} mol^{-1} were estimated from calorimetric measurements and used as fixed parameters for **4**. A quantitative light-induced excited spin state trapping (LIESST) effect was observed for **3**, and the high-spin to low-spin relaxation was studied in the temperature region 20–63 K.

Introduction

The chemistry of the triazole group has been investigated from the last part of the 19th century.[2] In particular, the coordinating ability of the 1,2,4-triazoles has been studied in depth and reviewed recently.[3] Metal complexes with 1,2,4-triazole and its derivatives afford a rich variety of monomeric, oligomeric, and one-, two-, and three-dimensional polymeric compounds with interesting physical, chemical, and structural properties. For a certain number of iron(II) complexes with 1,2,4-triazole-based ligands, the ligand field strength is close to the crossing point defined by the quintet (*S* = 2) high-spin state (HS) and the singlet (*S* = 0) low-spin state (LS). When the energy gap between both states is close to the thermal energy, population and depopulation of these states takes place. This behavior so-called spin crossover phenomenon can be triggered by a change of temperature or of

* To whom correspondence should be addressed. E-mail: jose.a.real@uv.es.
† Present addresses: V.N., Department of Chemistry, Memorial University, St. John's, NF, Canada A1B3X7; A.B.G., Institut für Anorganische und Analytische Chemie, Johannes Gutenberg Universität, Staudingerweg 9, D-55099 Mainz, Germany.
(1) (a) Institut de Ciencia Molecular/Departament de Química Inorgánica, Universitat de València. (b) Departament de Física Aplicada, Universitat Politécnica de València. (c) Departament de Química Orgánica, Universitat de València.
(2) Freund, F.; Meinecke, C. *Berichte* **1896**, *29*, 2486.
(3) Haasnoot, J. G. *Coord. Chem. Rev.* **2000**, *200–202*, 131.

Chart 1
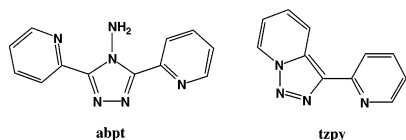
pressure or by irradiation with light.[4] The spin crossover phenomenon is an entropy-driven process; the entropic term compensates the energy gap which favors the LS ground state. Total entropy variation is the resultant of an electronic component arising from the difference of spin degeneracy of both spin states and a vibrational component.[5] Because of the antibonding character of the e_g orbitals, the average iron-to-ligand bond distance is around 0.2 Å larger in the HS state. Hence, the stretching force constant of the Fe−N bonds and also the energy gap between vibrational states are smaller in the HS state; consequently, vibrational entropy arises from the difference of vibrational states associated with the two spin states.

During the last 5 years, we have investigated the SCO phenomenon in the monomeric [Fe(abpt)$_2$(X)$_2$] system, where abpt is 4-amino-3,5-bis(pyridin-2-yl)-1,2,4-triazole (Chart 1) and X = NCS$^-$,[6] NCSe$^-$,[6] and [N(CN)$_2$]$^-$.[7] The NCS$^-$ and NCSe$^-$ derivatives form two polymorphs so-called A and B, which present slight structural differences.[6b,8] However, polymorph A undergoes spin transition whereas polymorph B is HS. The dicyanamide derivative displays a structure similar to that of the polymorph A and also undergoes spin transition. Investigation of the spin crossover conversion was carried out by magnetic, calorimetric, and photomagnetic studies on these derivatives. More recently, the magnetic properties of the NCS$^-$ derivative of polymorph B have been investigated as a function of temperature and pressure. Interestingly, this compound undergoes a spin conversion at 10.5 kbar similar to that observed for the polymoph A counterpart at 1 bar.[8]

Alternative ligands related to the 1,2,4-triazoles are interesting targets for investigating the SCO phenomenon. In this respect, we have recently focused on 3-(2-pyridyl)-[1,2,3]triazolo[1,5-a]pyridine (tzpy) (Chart 1). The chemistry of triazolopyridine compounds has been recently reviewed, the main observation with respect to their coordination chemistry being that the interaction of these ligands with

metals has been scarcely investigated.[9] In this paper we report for the first time the synthesis, X-ray single-crystal studies, and magnetic, photomagnetic, and calorimetric measurements of [Fe(tzpy)$_3$](BF$_4$)$_2$ (**1**), [Fe(tzpy)$_2$(NCS)$_2$]·S (S = 2CHCl$_3$ (**2**), H$_2$O (**3**)), and [Fe(tzpy)$_2$(NCSe)$_2$] (**4**).

Experimental Section

Materials. FeSO$_4$·7H$_2$O, Fe(BF$_4$)$_2$·6H$_2$O, KNCS, and KNCSe were purchased from commercial sources and used as received.

Preparation of the Ligand tzpy. When it was prepared as described,[10a] the yield was 26%. By manganese oxide oxidation of the intermediate hydrazone the yield was 86%,[10b] mp 125−127° (hexane/ethyl acetate) (lit. mp 123−125 °C (hexane/ethyl acetate)).

Preparation of [Fe(tzpy)$_3$](BF$_4$)$_2$ (1). A solution of tzpy in methanol/chloroform (2:1) (0.25 mmol, 10 mL) was added with stirring to a methanolic solution of [Fe(BF$_4$)$_2$]·6H$_2$O (0.085 mmol, 10 mL). The resulting solution was evaporated under an argon stream. After 3−4 days air-sensitive orange crystals were formed, filtered out, washed, and dried with argon. Yield: 30%. Anal. Calcd for C$_{33}$H$_{24}$N$_{12}$B$_2$F$_8$Fe: C, 50.81; H, 3.10; N, 21.55. Found: C, 51.26; H, 2.95; N, 22.03.

Preparation of [Fe(tzpy)$_2$(NCS)$_2$]·2CHCl$_3$ (2). The synthesis of **2** was performed by the slow diffusion method in a CHCl$_3$/H$_2$O solution and under argon atmosphere, with H-double-tube glass vessels. The starting materials were an aqueous solution of [Fe-(BF$_4$)$_2$]·6H$_2$O (0.1275 mmol, 5 mL) and KNCS (0.255 mmol, 5 mL) on one hand and a chloroform solution of tzpy (0.255 mmol, 5 mL) on the other. The H-double-tube was then filled with water. After 1 week, single crystals of **2** were collected and dried in an argon stream. Yield: 15%. Anal. Calcd for C$_{26}$H$_{18}$N$_{10}$Cl$_6$S$_2$Fe: C, 38.88; H, 2.26; N, 14.77. Found: C, 39.12; H, 2.45; N, 14.23.

Preparation of [Fe(tzpy)$_2$(NCX)$_2$]·S [X = S (S = H$_2$O) (3), Se (4)]. To a solution of FeSO$_4$·7H$_2$O (0.13 mmol) in methanol (20 mL) was added KNCX (X = S, Se) (0.25 nmol). A K$_2$SO$_4$ precipitate formed after stirring for 15 min was filtered off. To the resulting colorless solution containing Fe(II)/NCX$^-$ (1:2) was added a methanolic solution of tzpy (0.5 mmol, 25 mL). Orange crystalline solids of **3** and **4** were formed from the latter solution, after evaporation under an argon stream, in a few days. Yield: 20%. Anal. Calcd for C$_{24}$H$_{18}$N$_{10}$S$_2$OFe (**3**): C, 49.24; H, 3.47; N, 24.36. Found: C, 48.50; H, 3.10; N, 23.53. Anal. Calcd for C$_{24}$H$_{16}$N$_{10}$-Se$_2$Fe (**4**): C, 43.79; H, 2.45; N, 21.28. Found: C, 44.05; H, 2.33; N, 21.43.

Magnetic and Photomagnetic Measurements. The variable-temperature magnetic susceptibility measurements were carried out on samples constituted from small single crystals (20−30 mg) using a Quantum Design MPMS2 SQUID susceptometer equipped with a 5.5 T magnet and operating at 1 T and 1.8−300 K. The susceptometer was calibrated with (NH$_4$)$_2$Mn(SO$_4$)$_2$·12H$_2$O. Photomagnetic experiments were carried out using a Xe lamp with a 350−800 nm filter system coupled through an optical fiber to the SQUID susceptometer; the out power was 2 mW cm^{-2}. Experimental susceptibilities were corrected for diamagnetism of the constituent atoms by the use of Pascal's constants.

X-ray Crystallography. Single-Crystal Study. Diffraction data on prismatic crystals of **1** and **2** were collected at 293 K with an Enraf-Nonius CAD4 diffractometer using graphite-monochromated Mo Kα radiation (λ = 0.710 73 Å). The cell parameters were

(4) (a) Goodwin, H. A. *Coord. Chem. Rev.* **1976**, *18*, 293. (b) Gütlich, P. *Struct. Bonding (Berlin)* **1981**, *44*, 83. (c) Gütlich, P.; Hauser, A.; Spiering, H. *Angew. Chem., Int. Ed. Engl.* **1994**, *33*, 2024. (d) König, E.; Ritter, G.; Kulshreshtha, S. K. *Chem. Rev.* **1985**, *85*, 219. (e) König, E. *Struct. Bonding (Berlin)* **1991**, *76*, 51. (f) Lawthers, I.; McGarvey, J. J. *J. Am. Chem. Soc.* **1984**, *106*, 4280. (g) Decurtins, S.; Gütlich, P.; Hasselbach, K. M.; Spiering, H.; Hauser, A. *Inorg. Chem.* **1985**, *24*, 2174. (h) Decurtins, S.; Gütlich, P.; Köhler, C. P.; Spiering, H.; Hauser, A. *Chem. Phys. Lett.* **1984**, *105*, 1.

(5) Sorai, M.; Seki, S. *J. Phys. Chem. Solids* **1974**, *35*, 555.

(6) (a) Moliner, N.; Muñoz, M. C.; van Koningsbruggen, P. J.; Real, J. A. *Inorg. Chim. Acta* **1998**, *274*, 1. (b) Moliner, N.; Muñoz, M. C.; Létard, S.; Létard, J.-F.; Solans, X.; Burriel, R.; Castro, M.; Kahn, O.; Real, J. A. *Inorg. Chim. Acta* **1999**, *291*, 279.

(7) Moliner, N.; Gaspar, A. B.; Muñoz, M. C.; Niel, V.; Cano, J.; Real, J. A. *Inorg. Chem.* **2001**, *40*, 3986.

(8) Gaspar, A. B.; Muñoz, M. C.; Moliner, N.; Ksenofontov, V.; Levchenko, G.; Gütlich, P.; Real, J. A. *Monatsh. Chem.* **2003**, *134*, 285.

(9) Jones, G. *Adv. Heterocycl. Chem.* **2002**, *83*, 1.

(10) (a) Battaglia, L. P.; Carcelli, M.; Ferraro, F.; Mavilla, L.; Pellizzi, G. *J. Chem. Soc., Dalton Trans.* **1994**, 2651. (b) Abarca, B.; Ballesteros, R.; Elmasnaouy, M. *Tetrahedron* **1998**, *54*, 15287.

Table 1. Crystallographic Data for **1** and **2**

	1	**2**
empirical formula	$C_{33}H_{24}B_2F_8FeN_{12}$	$C_{26}H_{18}Cl_6FeN_{10}S_2$
fw	818.11	803.17
space group	Cc	$P\bar{1}$
a, Å	11.4680(6)	8.3340(4)
b, Å	27.449(2)	8.6520(4)
c, Å	12.4510(8)	11.6890(6)
α, deg		89.113(2)
β, deg	108.860(5)	81.612(2)
γ, deg		77.803(2)
V, Å^3	3709.0(4)	814.90(7)
Z	4	1
T, K	293(2)	293(2)
λ, Å	0.710 73	0.710 73
μ, mm^{-1}	0.490	1.120
ρ_{calc}, g/cm^3	1.465	1.637
R1^a	0.0930	0.0460
wR2^a	0.2521	0.0946

^{a} R1 $= \sum||F_o| - |F_c||/\sum|F_o|$; wR2 $= [\sum[w(F_o^2 - F_c^2)^2]/\sum[w(F_o^2)^2]]^{1/2}$. $w = 1/[\sigma^2(F_o^2) + (mP)^2 + nP]$, where $P = (F_o^2 + 2F_c^2)/3$, $m = 0.2000$ (**1**) and 0.0532 (**2**), and $n = 0.0000$ (**1**) and 0.0553 (**2**).

determined from least-squares refinement of 25 well-centered reflections in the range $12 < \theta < 20°$. Crystal parameters and refinement data are summarized in Table 1. Three standard reflections were monitored every 1 h, but no intensity variations were observed. Lorentz−polarization and absorption corrections were applied to the data. The structures were solved by direct methods using SHELXS97 and refined by the full-matrix least-squares method on F^2 using SHELXL97.[11] All non-hydrogen atoms were refined anisotropically.

Differential Scanning Calorimetry (DSC). Calorimetric measurements have been performed on **4** using a Mettler Toledo DSC 821^e differential scanning calorimeter. Low temperatures were obtained with an aluminum block attached to the sample holder, refrigerated with a flow of liquid nitrogen and stabilized at a temperature of 110 K. The sample holder was kept in a drybox under a flow of dry nitrogen gas to avoid water condensation. The measurements were carried out using around 20 mg of powdered sample sealed in aluminum pans with a mechanical crimp. Temperature and heat flow calibrations were made with standard samples of indium by using its melting (429.6 K, 28.45 J g^{-1}) transition. An overall accuracy of ±0.2 K in temperature and ±2% in the heat capacity is estimated. The uncertainty increases for the determination of the anomalous enthalpy and entropy due to the subtraction of an unknown baseline.

Results

Crystal Structure of 1 and 2. Compounds **1** and **2** crystallize in the Cc monoclinic and in the $P\bar{1}$ triclinic system, respectively. Table 2 gathers a selection of bond distances and angles for both compounds. Figure 1 displays the molecular structures of **1** and **2** together with the corresponding atomic numbering schemes. Compound **1** consists of discrete $[Fe(tzpy)_3]^{2+}$ cations and BF_4^- anions. The coordination sphere $[FeN_6]$, defined by the nitrogen atoms of the three α-diimine moieties of the tzpy ligands, corresponds to a slightly distorted octahedron, which binds through N(2), N(4), and N(6) atoms of the pyridine groups and N(1), N(3), and N(5) atoms of the triazole ring in a *mer*

(11) Sheldrick, G. M. *SHELXS97 and SHELXS97*; University of Göttingen: Göttingen, Germany, 1997.

Table 2. Selected Bond Distances (Å) and Angles (deg) for **1** and **2**^{a}

Compound **1**			
Fe−N(1)	1.887(8)	Fe−N(4)	1.994(10)
Fe−N(2)	1.982(11)	Fe−N(5)	1.968(8)
Fe−N(3)	1.963(12)	Fe−N(6)	1.949(13)
N(1)−Fe−N(2)	82.0(4)	N(2)−Fe−N(6)	90.5(4)
N(1)−Fe−N(3)	89.5(3)	N(3)−Fe−N(4)	79.3(4)
N(1)−Fe−N(4)	93.6(4)	N(3)−Fe−N(5)	93.5(5)
N(1)−Fe−N(5)	175.6(4)	N(3)−Fe−N(6)	173.3(5)
N(1)−Fe−N(6)	94.4(5)	N(4)−Fe−N(5)	90.1(4)
N(2)−Fe−N(3)	95.4(4)	N(4)−Fe−N(6)	95.0(4)
N(2)−Fe−N(4)	173.2(3)	N(5)−Fe−N(6)	82.9(3)
N(2)−Fe−N(5)	94.6(5)		

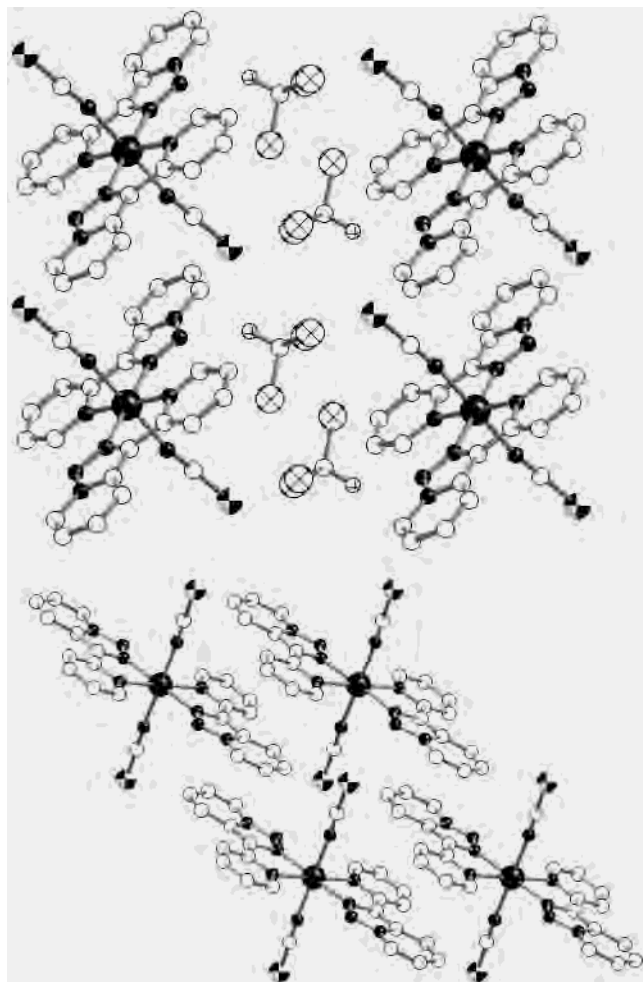| Compound **2**			
Fe−N(1)	2.211(2)	S(1)−C(12)	1.626(4)
Fe−N(2)	2.204(2)	N(3)−C(12)	1.155(4)
Fe−N(3)	2.113(3)		
N(1)−Fe−N(2)	75.14(10)	N(2)−Fe−N(3)	92.61(10)
N(1)−Fe−N(3)	89.88(10)	N(2)−Fe−N(2)^i	180.00(9)
N(1)−Fe−N(1)^i	180.0	N(3)−Fe−N(3)^i	180.00(11)
N(1)−Fe−N(2)^i	104.86(10)	N(2)−Fe−N(3)^i	87.39(10)
N(1)−Fe−N(3)^i	90.12(10)	N(3)−C(12)−S(1)	178.8(3)

^{a} Numbers in parentheses are estimated standard deviations in the least significant digit. Equivalent positions: i = $-x + 2$, $-y + 1$, $-z$.
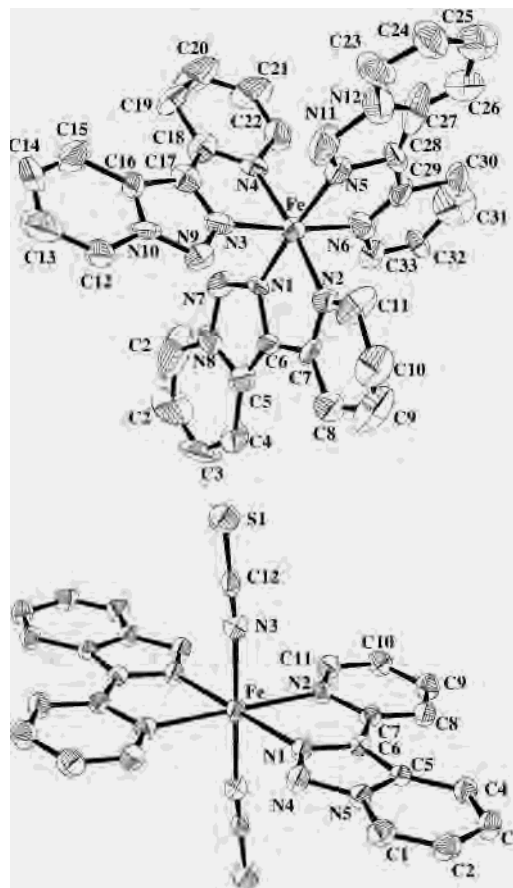
Figure 1. Perspective view of **1** (top) and **2** (bottom) at 293 K, including the non-hydrogen atom numbering. Thermal vibrational ellipsoids are at 40% probability level, and hydrogen atoms are omitted for clarity.

configuration. The Fe−N bond distances are Fe−N(1) = 1.887(8) Å, Fe−N(2) = 1.982(11) Å, Fe−N(3) = 1.963-(12) Å, Fe−N(4) = 1.994(10) Å, Fe−N(5) = 1.968(8) Å, and Fe−N(6) = 1.949(13) Å. These structural parameters

Figure 2. Crystal packing of **2**: (top) in the [100] direction illustrating the relative disposition of the complex and solvent layers; (bottom) in the [001] direction showing the π-interactions in a layer of complexes.

indicate the iron(II) ion is in the LS state in agreement with the magnetic measurements. The [Fe(tzpy)]₃²⁺ cations stack via π-interactions along the [100] and [101] directions; the voids defined by the cations are filled by the BF_4^- anions, which are strongly disordered.

Compound **2** consists of discrete neutral [Fe(tzpy)₂(NCS)₂] units and $CHCl_3$ solvent molecules. The iron(II) ion, lying in an inversion center, is coordinated to two tzpy ligands, which occupy the equatorial positions of a compressed octahedron. The axial positions are occupied by the NCS⁻ groups. The metal-to-ligand bond distances are Fe−N(1) = 2.211(2) Å, Fe−N(2) = 2.204(2) Å, and Fe−N(3) = 2.113(3) Å. These structural features indicate that the iron(II) ion is in the HS state at room temperature, according to the magnetic data. The NCS⁻ groups are almost linear with N(3)−C(12)−S(1) = 178.8(3)°. The molecules interact via π-stacking defining layers, the shortest C−C intermolecular distance being 3.458(4) Å. These layers are separated by sheets of $CHCl_3$, which stack along the *c* axis (see Figure 2).

Magnetic Behavior. The magnetic data for compound **1** indicate that iron(II) is in the LS state in the 2−300 K temperature range. The thermal dependence of the product
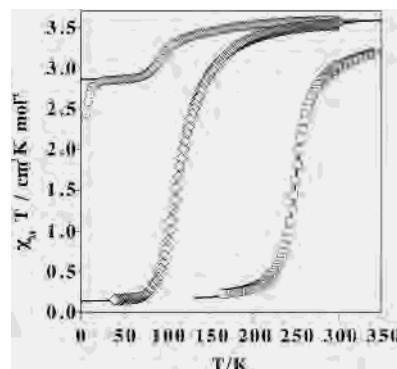
Figure 3. $\chi_M T$ versus *T* plots for **2** (circles), **3** (rhombuses), and **4** (squares). The solid line corresponds to simulation of the experimental spin conversion (see text).

$\chi_M T$ for **2−4** is displayed in Figure 3, χ_M being the molar magnetic susceptibility and *T* the temperature. At room temperature, $\chi_M T$ is equal to 3.6 cm³ K mol⁻¹ for **2**, which is in the range of the values expected for an iron(II) ion in the HS state. As the temperature is lowered, $\chi_M T$ first remains almost constant and then decreases more markedly from 120 to 70 K. The variation of $\chi_M T$, between 3.6 and 2.9 cm³ K mol⁻¹, corresponds to a very incomplete HS ↔ LS spin transition involving around 20% of iron(II) ions. The subsequent dropping of $\chi_M T$ at temperatures below 20 K corresponds most probably to the occurrence of zero-field splitting of the remaining HS ions. The $\chi_M T$ value at room temperature is 3.6 cm³ K mol⁻¹ for **3**. This value decreases first smoothly down to 250 K and then it drops sharply down 70 K to attain a value of 0.14 cm³ K mol⁻¹ indicating that the spin conversion is rather complete. The characteristic temperature at which 50% of conversion takes place, $T_{1/2}$, is 118 K for **3**. The magnetic behavior for **4** is similar to that of **3**, the main difference is that $T_{1/2} \approx 251$ K is shifted significantly toward higher temperatures. The $\chi_M T$ value is 3.2 cm³ K mol⁻¹ at 340 K and 0.2 cm³ K mol⁻¹ at 170 K. The spin conversions have been simulated, and the relevant thermodynamic parameters have been deduced from the expression (eq 1) derived from the regular solution model,[12]
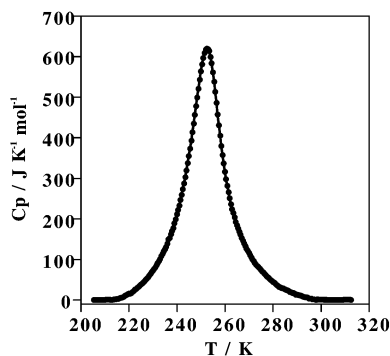
$$\ln[(1 - n_{HS})/(n_{HS} - f_{HS})] = [\Delta H + \Gamma(f_{HS} + 1 - 2n_{HS})]/RT - \Delta S/R \quad (1)$$

where ΔH, ΔS, and Γ are the enthalpy and the entropy variations and the parameter accounting for cooperativity associated with the spin conversion, respectively. The HS molar fraction, n_{HS}, has been deduced from the magnetic susceptibility through eq 2,

$$n_{HS} \approx (\chi_M T)_T/(\chi_M T)_{HS} \quad (2)$$

where $(\chi_M T)_T$ is the value of $\chi_M T$ at any temperature and $(\chi_M T)_{HS}$ corresponds to the pure HS state. In the present case $(\chi_M T)_{HS}$ has been considered an adjustable parameter. The parameter f_{HS} accounts for the HS molar fraction at low temperature (eq 3),

$$f_{HS} \approx (\chi_M T)_{LT}/(\chi_M T)_{HS} \quad (3)$$

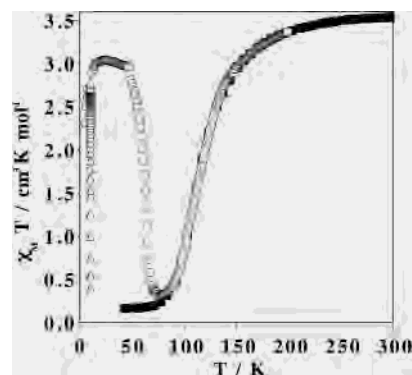**Figure 4.** Differential scanning calorimetric measurement of **4**.

Figure 5. $\chi_M T$ versus T plots for **3**. The sample was cooled from 300 to 10 K at 2 K min^{-1} (black squares), then irradiated (550 nm) for 150 min at 10 K (open triangles), and finally warmed from 4 to 200 K (0.5 K min^{-1}) after light irradiation was turned off.

Figure 6. Time dependence at various temperatures of the HS molar fraction, n_{HS}, generated by the LIESST effect. Solid lines represent the best fit to the experimental relaxation curves at different temperatures.

where $(\chi_M T)_{LT}$ corresponds to the value of $\chi_M T$ at low-temperature once the spin conversion has been accomplished. $\Delta H = 8.75$ kJ mol^{-1} and $\Delta S = 34.8$ J K^{-1} mol^{-1} have been estimated experimentally from calorimetric measurements (see below) and used as fixed parameters for **4**. Least-squares fitting led to $\Delta H = 3.67$ (**2**) and 4.08 (**3**) kJ mol^{-1}, $\Delta S = 34$ (**2**) and 34.5 (**3**) J K^{-1} mol^{-1}, $\Gamma = 0.86$ (**2**), 0.89 (**3**), and 3.79 (**4**) kJ mol^{-1}, and $(\chi_M T)_{HS} = 3.63$ (**2**), 3.76 (**3**), and 3.57 (**4**) cm^3 K mol^{-1}. These values are consistent with 100% and 95% of HS species at 300 K for **2** and **3**, respectively, and 89% of HS species at 340 K for **4**. The f_{HS} parameter indicates the occurrence of 80%, 4%, and 8% of HS species in the low-temperature region for **2**−**4**, respectively.

DSC Measurements for 4. The calorimetric measurements were carried out in the 120−340 K temperature range. A smooth line has been interpolated from the values in the normal regions, below 180 K and above 310 K. The heat capacity due to the transition has been deduced by subtraction of this baseline. The temperature dependence of the anomalous heat capacity, ΔC_p, in the heating mode for **4** is in Figure 4. The temperatures of the maxima of the heat capacity curves were obtained for heating and cooling thermograms measured at different rates. The extrapolation at zero rate gave the same transition temperature on heating and cooling without any noticeable hysteresis. The critical temperature, $T_{1/2}$, has been obtained from the maximum of ΔC_p vs T, after correcting for the heating and cooling thermal lags. We found $T_{1/2} = 252$ K for **4**. This value agree rather well with that observed from the $\chi_M T$ vs T plot. The overall enthalpy (ΔH) and entropy (ΔS) variation associated with the spin transition determined from the DSC curves is $\Delta H = 8.75 \pm 0.4$ kJ mol^{-1} and $\Delta S = 34.8 \pm 3$ J K^{-1} mol^{-1}.

Photomagnetic Measurements. Photogeneration of the metastable HS state at low temperatures, the so-called light-induced excited spin state trapping experiment (LIESST), was carried out on a microcrystalline sample (0.72 mg) of **3**. The results are displayed in Figure 5. The magnetic response was measured first in the cooling mode (cooling rate 2 K min^{-1}) from 300 to 10 K with an applied magnetic field of 1.5 T (closed circles). At 10 K, the sample was irradiated with green light (550 nm) for 150 min, the time required to attain the saturation value of $\chi_M T \approx 3.0$ cm^3 K mol^{-1} (closed triangles). The light irradiation was then switch
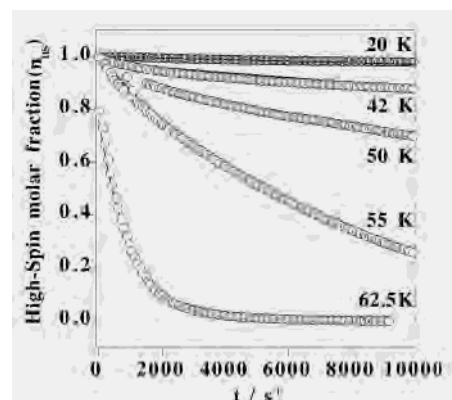
off, and temperature was first decreased to 4 K and then increased to 200 K at the rate of 0.5 K min^{-1}. In the 4−25 K region the increase of $\chi_M T$ is consistent with the thermal population of the different microstates arising from zero-field splitting of the $S = 2$ state. In the temperature range 25−50 K, $\chi_M T$ is almost constant with a value around 3.0 cm^3 K mol^{-1} indicating that ca. 100% of molecules have been converted to the metastable HS state. At temperatures greater than 50 K, $\chi_M T$ drops rapidly to reach a value close to 0.14 cm^3 K mol^{-1}, at 78 K indicating the occurrence of a complete HS → LS relaxation. At temperatures greater than 85 K, $\chi_M T$ increases again following the conversion observed on the cooling mode. The characteristic temperature corresponding to the maximum variation of $\chi_M T$ in the HS → LS relaxation after LIESST, T_{liesst},[13] is ca. 71 K.

The dynamics of the HS → LS relaxation was investigated in the temperature range 20−63 K. For higher temperatures, relaxation was to fast relative to the SQUID time window. The decay of the LIESST-generated HS species at various temperatures is displayed in Figure 6. A single-exponential law was used for simulating the data according to the expression

$$n_{HS} = \exp[(-k_{HL}(T))t] \qquad (4)$$

where $k_{HL}(T)$ corresponds to the relaxation rate at temperature T. The best simulation was obtained for the $k_{HL}(T)$ values 1

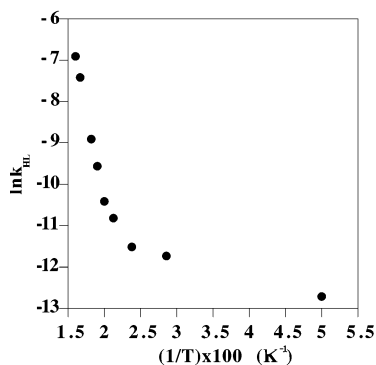(12) Slichter, C. P.; Drickamer, H. G. *J. Chem. Phys.* **1972**, *56*, 2142.

Figure 7. $\ln[k_{HL}(T)]$ versus $1/T$ Arrhenius plot for **3**.

$\times 10^{-3}$, 6×10^{-4}, 1.35×10^{-4}, 7.0×10^{-5}, 3×10^{-5}, 2×10^{-5}, 1×10^{-5}, 8×10^{-6}, and 3×10^{-6} s^{-1} for $T = 62.5$, 60, 55, 52.5, 50, 47, 42, 35, and 20 K, respectively. The corresponding Arrhenius plot $\ln[k_{HL}(T)]$ vs $1/T$ has been depicted in Figure 7. Two main regions can be observed, one at relative high temperatures where $k_{HL}(T)$ shows a strong T-dependence and the other where $k_{HL}(T)$ is very small and almost temperature independent.[14] In the whole investigated temperature region both thermally activated and tunneling deactivation mechanisms play important roles, which cannot be decoupled. At temperatures below 50 K, a pure tunneling mechanism is predominant. A consequence of this behavior is that the kinetic parameters deduced from the Arrhenius law, preexponential factor and activation energy, are far from realistic.

Discussion and Conclusion

In this paper we have reported the synthesis and characterization of new mononuclear spin crossover compounds based on the ligand tzpy. Compound **1** is made up of mononuclear units where the iron(II) atom is surrounded by six nitrogen atoms belonging to three tzpy ligands. The average Fe−N bond distance, 1.957(10) Å, is similar to that observed for other tris(α-diimine)iron(II) complexes like, for instance, [Fe(bpym)$_3$](ClO$_4$)$_2$·1/4H$_2$O (bpym is 2,2′-bipyrimidine), whose average Fe−N bond distance is 1.97(5) Å.[15] The short metal-to-ligand bond distances indicate that the iron(II) atom is in the LS state at room temperature according to the magnetic measurements. However, it should be noted that the related 1,2,4-triazole compounds [Fe(L)$_3$](anion)$_2$-(solvent)$_x$, where L is 3-(pyridin-2-yl)-1,2,4-triazole [anion = Cl$^-$, ClO$_4^-$, PF$_6^-$, BF$_4^-$; solvent = ethanol, water][16−18] or 3-methyl-5-(pyridin-2-yl)-1,2,4-triazole [anion = ClO$_4^-$, PF$_6^-$; solvent = water][19] undergo spin crossover behavior in contrast to **1**. For instance, the average Fe−N bond

distance is 2.178(4) and 2.027(3) Å at 250 and 95 K, temperatures at which the compound is fully HS and LS (with 30% residue HS), respectively.[18]

Substitution of one tzpy chelate ligand by two weaker monodentate pseudohalide groups NCS$^-$ or NCSe$^-$ afforded the new spin crossover compounds **2−4**. The crystal structure of **2** shows that the two tzpy ligands and NCS$^-$ groups adopt a configuration trans. The former occupy the equatorial plane, and the latter, the axial positions of the coordination octahedron. The coordination modes of tzpy are similar to those reported by Battaglia et al.[10a] in [Cu(tzpy)$_2$(H$_2$O)$_2$]-(NO$_3$)$_2$ where the axial positions of the copper(II) ion are occupied by two water molecules instead of two NCS$^-$ groups. The crystal structure of **2** also shows a remarkable similarity with that of the polymorphs A and B of the compound [Fe(abpt)$_2$(NCS)$_2$]. The Fe−N bond distances are Fe−N(pyridine) = 2.205(5) Å, Fe−N(triazole) = 2.120(4) Å, and Fe−NCS = 2.120(5) Å for polymorph A.[6b] The corresponding average bond distance, 2.148(5) Å, is 0.028 Å shorter than that of **2**. On the basis of the consideration that the ligand field strength, Δ_0, is proportional to $1/r^6$ (r being the average Fe−N bond distance), the Δ_0 originated in **2** is estimated to be 8% smaller than in the abpt derivative. This fact is consistent with the critical temperatures, $T_{1/2}$, 108 and 184 K observed for **2** and abpt derivative (polymorph A), respectively. It is interesting to point out that the polymorph B of the abpt derivative has virtually the same average Fe−N bond distance, 2.171(5) Å, as **2**. Despite this fact, the polymorph B is HS in the whole temperature range at 1 bar. However, an incomplete spin transition (estimated $T_{1/2} \approx 75$ K) is observed at 4.4 kbar whereas a complete conversion is achieved at 5.6 kbar ($T_{1/2} = 107$ K).[8] Pressure increases the intermolecular interactions and consequently makes shorter the Fe−N distances, which induce an increase of the ligand field strength.

The distinct spin crossover behavior observed for the solvates CHCl$_3$ and H$_2$O of [Fe(tzpy)$_2$(NCS)$_2$] with $T_{1/2} = 108$ K (**2**) and 118 K (**3**), respectively, may be ascribed to small differences in the average Fe−N bond distances stemming from the different crystal packing expected for both solvates. The uncommon high-temperature shift observed for $T_{1/2}$ when moving from **3** to **4**, $\Delta T_{1/2} \approx 145$ K, cannot be explained only in terms of the ligand field strength generated by the groups NCS$^-$ (**3**) and NCSe$^-$ (**4**). It is well-known that the smaller electronegativity of the NCSe$^-$ group compared to that of the NCS$^-$ group makes the ligand field strength of the former slightly stronger. This fact is reflected in the Fe−N distances, being shorter for the NCSe$^-$ derivatives. For this reason $T_{1/2}$ shifts ca. 20−50 K to higher temperatures when replacing NCS$^-$ by NCSe$^-$ (see for instance refs 5 and 6b). Hence, the shift $\Delta T_{1/2} \approx 145$ K most likely is the resultant of two components, one small due to

(13) Létard, J. F.; Capes, L.; Chastanet, G.; Moliner, N.; Létard, S.; Real, J. A.; Kahn, O. *Chem. Phys. Lett.* **1999**, *313*, 115.
(14) (a) Buhks, E.; Navon, G.; Bixon, M.; Jortner, J. *J. Am. Chem. Soc.* **1980**, *102*, 2918. (b) Beattie, J. K. *Adv. Inorg. Chem.* **1988**, *32*, 2. (c) Xie, C. L.; Hendrickson, D. N. *J. Am. Chem. Soc.* **1987**, *109*, 6981. (d) Hauser, A. *Comments Inorg. Chem.* **1995**, *17*, 17. (e) Hauser, A.; Jeftic, J.; Romstedt, H.; Hinek, R.; Spiering, H.; Gütlich, P. *Coord. Chem. Rev.* **1999**, *190−192*, 471.
(15) De Munno, G.; Julve, M.; Real, J. A. *Inorg. Chim. Acta* **1997**, *255*, 185.
(16) Stupik, P.; Zhang, J. H.; Kwiecien, M.; Reiff, W. M.; Haasnoot, J. G.; Hage, R.; Reedijk, J. *Hyperfine Interact.* **1986**, 725.

(17) Stupik, P.; Reiff, W. M.; Hage, R.; Jacobs, J.; Haasnoot, J. G.; Reedijk, J. *Hyperfine Interact.* **1988**, 343.
(18) Stassen, A. F.; Vos, M.; van Koningsbruggen, P. J.; Renz, F.; Ensling, J.; Kooijman, H.; Speck, A. L.; Haasnoot, J. G.; Gütlich, P.; Reedijk, J. *Eur. J. Inorg. Chem.* **2000**, 2231.
(19) Sugiyarto, K. H.; Craig, D. C.; Rae, A. D.; Goodwin, H. A. *Aust. J. Chem.* **1995**, 35.

the change of the ligand field strength associated with the change of pseudohalide ligand and another more important related with the difference in crystal packing expected for **3** and **4**.

The thermodynamic parameters estimated from the magnetic and calorimetric data are quite reasonable as compared with those previously reported for iron(II) spin crossover complexes. The value of ΔS is greater than the electronic spin change expected for a iron(II) ion $\Delta S_{spin} = R \ln [(2S + 1)HS/(2S + 1)LS] = 13.45$ J K^{-1} mol^{-1}. The remainder entropy variation, 21 J K^{-1} mol^{-1}, is mainly due to the intramolecular vibrational changes.[5,20−22] It should be noted that the calculated Γ values account for the poor cooperativity observed for the three derivatives as $\Gamma < 2RT_{1/2}$.[12]

Observation of important amounts of trapped HS molecules at low temperatures is usually ascribed to the occurrence of two different sites in the crystal.[23] One site imparts weaker ligand field strength and, consequently, stabilizes HS molecules whereas the other, with a stronger ligand field, stabilizes spin crossover centers. Texture effects or occurrence of different polymorphs, one of them being paramagnetic in the whole range of temperatures, has been also claimed.[4d] Further, for spin transition taking place at very low temperature a frozen-in effect have been reported.[7] In such a situation the spin crossover species have no thermal energy to overcome the activation energy barrier, which accompanies the HS ↔ LS transformation. We believe that the latter is the most plausible explanation for the occurrence of only 20% of spin conversion in **2**. The frozen-in effect is not uncommon in the field of iron(II) spin crossover phenomenon, and for instance, it has been described for the related compounds {[Fe(abpt)$_2$[(N(CN)$_2$]$_2$}[7] and [Fe(abpt)$_2$-(NCS)$_2$].[8]

Finally, from the photomagnetic experiments we have demonstrated that **3** shows an almost quantitative LIESST effect with a characteristic temperature $T_{liesst} = 71$ K at which the relaxation back rate from the HS to the LS is maximum. Below 71 K time evolution of $\chi_M T$ is exponential according to the poor cooperativity observed in the system. Dynamics of the HS → LS relaxation is strongly influenced by the tunneling mechanism, even at 62.5 K, which makes impossible a proper evaluation of the characteristic Arrhenius parameters, preexponential factor and activation energy barrier, in the temperature region studied.

Supporting Information Available: X-ray crystallographic files for [Fe(tzpy)$_3$](BF$_4$)$_2$ and [Fe(tzpy)$_2$(NCS)$_2$]·2CHCl$_3$ in CIF format. This material is available free of charge via the Internet at http://pubs.acs.org.

IC034366Z

(20) Bousseksou, A.; McGarvey, J. J.; Varret, F.; Real, J. A.; Tuchagues, J. P.; Dennis, A. C.; Boillot, M. L. *Chem. Phys. Lett.* **2000**, *318*, 409.
(21) Moliner, N.; Salmon, L.; Capes, L.; Muñoz, M. C.; Létard, J. F.; Bousseksou, A.; Tuchagues, J. P.; McGarvey, J. J.; Dennis, A. C.; Castro, M.; Burriel, R.; Real, J. A. *J. Phys. Chem B* **2002**, *106*, 4247.
(22) Molnár, G.; Niel, V.; Gaspar, A. B.; Real, J. A.; Zwick, A.; Bousseksou, A.; McGarvey, J. J. *J. Phys. Chem B* **2002**, *106*, 9701.
(23) (a) Wiehl, L. *Acta Crystallogr.* **1993**, *B49*, 289. (b) Poganiuch, P.; Decurtins, S.; Gütlich, P. *J. Am. Chem. Soc.* **1990**, *112*, 3270. (c) Buchen, T.; Poganiuch, P.; Gütlich, P. *J. Chem. Soc., Dalton Trans.* **1994**, 2285. (d) Hinek, R.; Spiering, H.; Schollmeyer, D.; Gütlich, P.; Hauser, A. *Chem.—Eur. J.* **1996**, *2*, 1127.